

Molecular dynamics simulation of the soft mode for hydrogen-bonded ferroelectrics

D. Merunka and B. Rakvin

Ruder Bošković Institute, P.O. Box 180, 10002 Zagreb, Croatia

(Received 3 May 2002; revised manuscript received 9 August 2002; published 6 November 2002)

Numerical simulations of dipole dynamics have been studied by employing a recently proposed modified strong dipole proton coupling (MSDPC) model of the phase transition in the hydrogen-bonded type of ferroelectrics. The obtained results in the form of the spectral density of the polarization fluctuation along the polar axis and along the lateral direction are simulated and correlated with known experimental data obtained primarily by Raman and infrared spectroscopy on KDP and DKDP lattices. A central peak (CP) appears in the calculated spectral density of the longitudinal polarization fluctuation in the ferroelectric phase of KDP and DKDP. The simulated CP indicates an order-disorder mechanism of excitation in the paraelectric phase near T_c in both crystals. By increasing the temperature to 460 K, the crossover to the displacive behavior for KDP lattice is predicted. The model also predicts a low-frequency flat anomaly for KDP and a CP for DKDP in the spectral density of transversal polarization fluctuations, as was earlier detected by infrared and Raman spectroscopy. The superiority of the MSDPC model is additionally tested in the description of the experimentally obtained pressure-induced change of the CP line shape for KDP.

DOI: 10.1103/PhysRevB.66.174101

PACS number(s): 77.84.Fa

I. INTRODUCTION

The mechanism of the ferroelectric phase transition in KH_2PO_4 -type ferroelectrics (KDP) is not yet fully explained.^{1,2} One of the peculiar properties, which is not easy to incorporate in the model, is a description of the simple H \rightarrow D isotope exchange effect on the phase transition temperature T_c . Thus, a large shift of T_c from 122 K to 225 K, due to isotope exchange, appears to be one of the most powerful tests for the quality of the proposed model.

The first widely accepted model offering a solution for this problem, based on proton tunneling in the double-minimum potential, was proposed by Blinc.³ The large increase of T_c caused by the exchange effect is explained by the difference of tunneling frequency due to the mass difference between proton and deuteron. In the suggested tunneling model the collective tunneling motion coupled with the polar phonon mode softens to trigger the phase transition. The low-frequency polar mode was later detected as an intense central peak (CP) in the Raman spectrum⁴ and has been interpreted as a ferroelectric overdamped soft mode coupled with the collective proton tunneling mode. Thus, in such a tunneling model the phase transition is of a displacive type with a softening of the optical phonon mode. There are several experimental results which are inconsistent with this model that were discussed in detail.² Following this discussion one finds that there is no strong experimental evidence for such a proton tunneling mode from the neutron scattering data and, in addition, the polar mode is heavily overdamped even at room temperature where an underdamped soft mode is expected.

It should be noted that in the Raman spectra it is difficult to distinguish between an overdamped oscillatory soft mode, which comes from a displacive model, and a relaxational mode, characteristic of an order-disorder model, due to similar spectrum shapes in the frequency domain. Therefore, Tominaga and Urabe⁵ suggested an additional interpretation for the CP observed in the B_2 symmetry Raman spectrum

based on an order-disorder model. In the newly proposed model, the CP is assumed to be composed of two parts: a polarization fluctuation mode and a libration mode of PO_4 tetrahedra. Moreover, the additional experimental data obtained later by far-infrared reflectivity⁶ and impulsive stimulated Raman scattering⁷ support order-disorder phase transition. However, it should be noted that the explanation for a physical origin of exchange effects was not included in the model.

Recently Sugimoto and Ikeda⁸ proposed a strong dipole-proton coupling (SDPC) model with a large isotope effect on the transition temperature without including the tunneling motion of protons. In the SDPC model the isotope effect is due to the difference in ground-state energies between proton and deuteron in the potential of the hydrogen bond affected by the ordering of the dipole moments (induced by distortion of PO_4 tetrahedra). A new improvement of the SDPC model was also recently suggested⁹ by introducing continuous three-dimensional changes of the dipole instead of one-dimensional changes only along the c axis, as was considered in the original SDPC model. The influence of the introduced modifications on the ferroelectric phase transition was examined by employing a Monte Carlo calculation.⁹ It is shown that the spontaneous polarization along the polar c axis in the vicinity of T_c is better described with the modified SDPC (MSDPC) model than with the original SDPC model. The additional superiority of the MSDPC model compared to the original model is the ability to describe the discontinuity in the transversal dielectric constant around T_c . Moreover, it is also shown that the MSDPC model reduces a gap between the previously calculated and experimentally detected shift of T_c for the isotopic exchange effect.

The efficiency of the MSDPC model to predict the isotope effect in T_c and transversal dielectric constant anomaly suggests that it can be used for a more detailed description of phase transition in KDP lattices. In this work the MSDPC model will be employed to examine the dynamic properties of the phase transition in hydrogen bonding ferroelectrics.

The Langevin equations, with potential derived from the MDSPC model, are used in numerical calculations of the longitudinal and transversal polarization dynamics in KDP and DKDP crystal lattices. In the calculated longitudinal polarization fluctuation spectra, a CP appears and increases by reaching T_c from below. Above and near T_c , the CP also dominates the spectra and gives us an opportunity for a detailed study of the dynamic mechanism in the vicinity of T_c . Moreover, together with expected peaks, transversal polarization fluctuation spectra also show a flat low-frequency anomaly for KDP and CP for DKDP. All these results will be discussed and correlated with experimental data.

II. MODEL AND COMPUTATIONAL DETAILS

The calculation and simulation procedure will be provided in two steps. The H (D) ground-state energy terms in the potential energy of the dipole system have nonlinear form and an analytical approach to the problem is possible only near $T=0$ K. Thus, in the first step, a harmonical approximation of the equations of motion will be applied and dynamical parameters for the lowest longitudinal (polarized along c) and transversal (polarized along a, b) modes will be calculated. In order to study the polarization dynamics in a wide temperature range (up to 460 K), numerical integration of the classical Langevin equations will be undertaken in the second step.

Before starting to simulate the dynamics of dipole moments by employing the model, the main characteristics of the model can be briefly summarized. In the MDSCP model a unit PO_4 dipole in the three-dimensional hydrogen bond network such as KDP is not directed only along c axis and can be described as a vector $\boldsymbol{\mu}_i = (\mu_i^a, \mu_i^b, \mu_i^c)$ with components along the crystal axis (a, b, c). In the SDPC model, the proton position and ground-state energy directly depend on the interaction with the two neighbor dipoles and it is described as the force $F = K(\mu_i + \mu_j)$ along the oxygen-hydrogen-oxygen bond with a constant of proportionality, K . An additional new constant of proportionality, K_\perp , has been introduced in the MDSCP model to describe the transversal dipole interaction. The new form of the force $F_{i',\rho}$ which acts on H (D) was obtained earlier [Eq. (1) in Ref. 9]. In a similar way the parameters of elastic deformation energy, A and A_\perp , are introduced into the potential energy given for the system of N dipoles and $2N$ hydrogen bonds:

$$E_{pot} = \sum_{i=1}^N \left[\frac{A_\perp}{2} (\mu_i^{a2} + \mu_i^{b2}) + \frac{A}{2} \mu_i^{c2} \right] - \sum_{i'=1}^{N/2} \sum_{\rho=1}^4 (\sqrt{h^2 + I^2 F_{i',\rho}^2} - h). \quad (1)$$

The first term describes the elastic deformation energy ($A, A_\perp > 0$) of the tetrahedra for an induction of dipoles in the arbitrary direction and the second term describes the ground-state energy of $2N$ protons or deuterons. The parameter h describes the effect of mass (H or D) and the geometric effect while the parameter I is approximately the same for both lattices.^{8,9}

TABLE I. Evaluated parameters for the longitudinal polarization by employing the characteristic constants $h^H = 110$ meV, $\mu_s^H = 4.8 \times 10^{-30}$ C m, and $t_0 = 2 \times 10^{-14}$ s.

	f_0 $h^H/(\mu_s^H)^2$	f_1 $h^H/(\mu_s^H)^2$	M $t_0^2 h^H/(\mu_s^H)^2$	ω_{FE} (cm^{-1})	ω_{AFE} (cm^{-1})
KDP	1.46	-0.09	3.405	150	195
DKDP	1.74	-0.03	3.405	184	195

For a description of the dynamics behavior of N dipoles in the ferroelectric phase (near $T=0$ K), the same classical approximation to the motion of dipole moments has been used as in the SDPC model^{10,11} and can be represented by the following equations:

$$M_\perp \frac{d^2 \mu_i^a}{dt^2} = - \frac{\partial E_{pot}}{\partial \mu_i^a},$$

$$M_\perp \frac{d^2 \mu_i^b}{dt^2} = - \frac{\partial E_{pot}}{\partial \mu_i^b}, \quad i = 1, \dots, N, \quad (2)$$

$$M \frac{d^2 \mu_i^c}{dt^2} = - \frac{\partial E_{pot}}{\partial \mu_i^c}.$$

As can be noted here, the two additional equations are added in the MDSCP model and it is expected that the effective mass of the dipole moment in the transverse direction M_\perp differs from the effective mass M along the c axis. Following a procedure similar to that done earlier,¹⁰ it is expected that in the ferroelectric phase (near $T=0$ K) most of the dipole moments differ slightly from the saturated dipole (dipole directed along the c axis with saturated value μ_s). The linearized equations of motion are obtained by expanding the right-hand sides of Eq. (2) to a linear term in the small deviations of the dipole from the saturated one. The six modes of the dipole moment wave, with wave vector \mathbf{k} , appear as solutions for two dipoles per unit cell. The problem is simplified for the center of Brillouin zone ($\mathbf{k}=0$) where the longitudinal mode (along c) and transversal mode (along a, b) are decoupled.

The two longitudinal modes are the ferroelectric and antiferroelectric mode with frequencies $\omega_{FE} = \sqrt{(f_0 + 4f_1)/M}$ and $\omega_{AFE} = \sqrt{(f_0 - 4f_1)/M}$. The force constants f_0 and f_1 have the same meaning as in the SDPC model, but their values are different in the MSDPC model and they are calculated from the MSDPC parameters (Table I in Ref. 9) and presented in Table I. The value for the effective mass M is adjusted so that the ferroelectric mode frequency ($\omega_{FE} = 150 \text{ cm}^{-1}$ for KDP) has the same value as the frequency of the lowest experimentally detected A_1 mode (S mode).^{12,14} This value of M leads to the longitudinal mode frequencies in KDP and DKDP as shown in Table I.

The four additional new modes obtained inside the MSDPC model are related to the transversal dipole dynamics. It

TABLE II. Evaluated parameters for the transversal polarization by employing the characteristic constants $h^H=110$ meV, $\mu_s^H=4.8 \times 10^{-30}$ C m, and $t_0=2 \times 10^{-14}$ s.

	f_0^\perp $h^H/(\mu_s^H)^2$	f_1^\perp $h^H/(\mu_s^H)^2$	M_\perp $t_0^2 h^H/(\mu_s^H)^2$	ω_- (cm^{-1})	ω_+ (cm^{-1})
KDP	0.091	-0.009	0.508	100	123
DKDP	0.105	-0.003	0.508	117	123

can be noted that two degenerate low-frequency modes $\omega_- = \sqrt{(f_0^\perp + 2f_1^\perp)/M_\perp}$ involve the motion of protons while the other two high-frequency degenerated modes, $\omega_+ = \sqrt{(f_0^\perp - 2f_1^\perp)/M_\perp}$ appear without proton motion. The modes polarized in a direction perpendicular to the c axis are expected to be detected in the infrared reflectivity spectroscopy as well as in Raman spectroscopy with B_1 and B_2 symmetry species in the ferroelectric phase (FE). Indeed, in the low infrared spectroscopy of KDP several peaks at 100, 118, 131.5, 180, and 242 cm^{-1} , assigned as three translation modes of K-PO_4 and two libration modes of PO_4 , can be found in the FE phase.¹⁵ Since there is no additional information to obtain a more accurate correlation between these five experimental and two calculated modes, the effective mass M_\perp is adjusted to reproduce the lowest-frequency mode $\omega_- = 100$ cm^{-1} . Values for transversal force constants f_0^\perp and f_1^\perp , together with transversal mode frequencies, were calculated from the MSDPC parameters⁹ and are given in Table II. Smaller values of transversal effective dipole mass and transversal force constants compared to their longitudinal counterparts are obtained by adapting the lowest-frequency mode together with the value of the transversal dielectric constant ($\epsilon_a \sim 59$ at 140 K).

The peak positions of ω_{FE} in KDP and DKDP (Table I) show an expected isotope effect. One notes that the peak position in DKDP is at a frequency 1.23 times higher than that of KDP. This is in accordance with Raman spectroscopy data for the S mode¹⁴ (for KDP, $\omega = 142$ cm^{-1} at $T = 100$ K, and for DKDP, $\omega = 165$ cm^{-1} at 213.6 K). The obtained values for antiferroelectric (AFE) modes [$\omega_{AFE} = 195$ cm^{-1} (Table I)] are in closer vicinity to the experimentally measured antiferroelectric modes (114, 160, and 214 cm^{-1}) (Ref. 16) than the same frequency calculated for the SDPC model ($\omega_{AFE} = 73$ cm^{-1}).

For the study of the motional dynamics of N dipoles in the vicinity of the phase transition, a more rigorous treatment, beyond the linear approximation, is required because the nonlinearity of the equations becomes important. The long-range part of the direct interaction between dipole moments is expected to induce fluctuations of the dipole moments. Thus, these effects can be described by employing a set of Langevin equations in terms of stochastic forces and damping,

$$M_\perp \frac{d^2 \mu_i^a}{dt^2} = -\frac{\partial E_{pot}}{\partial \mu_i^a} - \Gamma_0 M_\perp \frac{d \mu_i^a}{dt} + F_i^a(t)$$

$$M_\perp \frac{d^2 \mu_i^b}{dt^2} = -\frac{\partial E_{pot}}{\partial \mu_i^b} - \Gamma_0 M_\perp \frac{d \mu_i^b}{dt} + F_i^b(t), \quad i = 1, \dots, N, \quad (3)$$

$$M \frac{d^2 \mu_i^c}{dt^2} = -\frac{\partial E_{pot}}{\partial \mu_i^c} - \Gamma_0 M \frac{d \mu_i^c}{dt} + F_i^c(t),$$

where $F_i(t)$ and Γ_0 are the stochastic force and damping constant, respectively. The behavior of stochastic forces is determined by condition

$$\langle F_i^\alpha(0) F_j^\beta(t) \rangle = 2\Gamma_0 M_\alpha k T \delta_{ij} \delta_{\alpha\beta} \delta(t). \quad (4)$$

Following this condition for $F_i^\alpha(t)$, the temperature of the system, T , is kept at a constant value.

In the simulation, a unit cell corresponds to the tetragonal unit cell of the crystal with four PO_4 tetrahedra. A model system is the three-dimensional (3D) supercell, which consists of $2 \times 2 \times 2$ unit cells. Simulation of the dipole dynamics is calculated for such model system of $N=32$ PO_4 dipoles by imposing periodic boundary conditions and using a Verlet algorithm.¹⁷ The stochastic force acting on the dipole moment holds at a constant value over the time interval $\Delta t = t_0/2$. The integration step (0.5×10^{-14} s) and time interval (1×10^{-14} s) are shorter than the fastest oscillation in the system ($\sim 20.0 \times 10^{-14}$ s). It is convenient to introduce dimensionless variables proportional to a and c polarization,

$$s_a(t) = \frac{1}{N \mu_s^H} \sum_{i=1}^N \mu_i^a(t),$$

$$s_c(t) = \frac{1}{N \mu_s^H} \sum_{i=1}^N \mu_i^c(t), \quad (5)$$

and to define spectral density functions which are proportional to experimentally measured Raman spectral intensities:

$$G(s_c, \omega) = \frac{1}{2\pi} \int_{-\infty}^{\infty} \langle [s_c(0) - \langle s_c \rangle] [s_c(t) - \langle s_c \rangle] \rangle e^{i\omega t} dt,$$

$$G(s_a, \omega) = \frac{1}{2\pi} \int_{-\infty}^{\infty} \langle s_a(0) s_a(t) \rangle e^{i\omega t} dt. \quad (6)$$

It can be noted that in the simulation procedure the damping constant remains as the one unknown and temperature-independent parameter.

III. RESULTS AND DISCUSSION

The molecular dynamics simulations have been performed by employing classical Langevin equations. Spectral densities were evaluated in the wide temperature interval around T_c . The phase transition is obtained in the vicinity of 130 K and coincides with earlier Monte Carlo calculations of T_c . Temperature dependences of the spectral densities, $G(s_c, \omega)$, calculated for the damping constant ($\Gamma_0 = 26.5$ cm^{-1}) in the FE phase and in the paraelectric (PE)

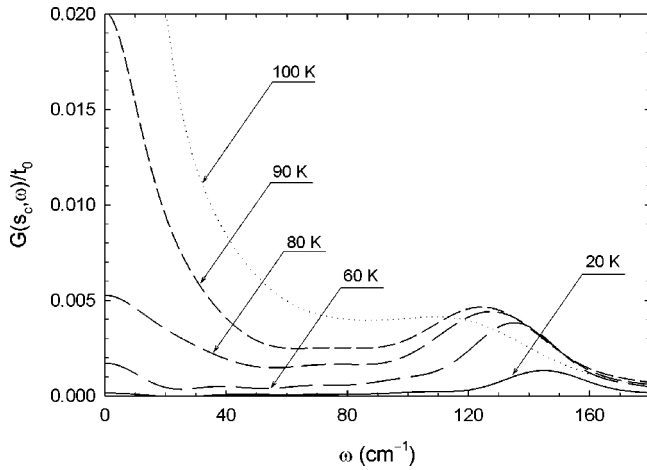


FIG. 1. Spectral densities calculated for $\Gamma_0=26.5 \text{ cm}^{-1}$ along the polar axis of KDP at several temperatures in the ferroelectric phase.

phase of KDP are shown in Figs. 1 and 2. The choice of the damping constant value was taken in accordance with the medium damping ($\beta/\beta_0=0.1$) case which was suggested earlier.¹¹ As is expected in the low-temperature region only one inelastic peak from the oscillatory mode at 150 cm^{-1} can be seen. This peak exhibits a shift towards lower frequencies with an increase of the damping constant at higher temperatures. An additional CP is also present in the FE phase. The intensity of the CP strongly increases as $T \rightarrow T_c$ for $T < T_c$. In the PE phase, only one broad inelastic peak at around 70 cm^{-1} is obtained at high temperature, near $T = 460 \text{ K}$. Below 380 K , this peak transforms into CP-type and its intensity increases as $T \rightarrow T_c$ for $T > T_c$. It is known⁴ that the longitudinal polarization modes can be compared with well-known $B_2(z)$ Raman spectra of KDP in the configuration $X(YX)Y$ for the PE phase and with $A_1(z)$ in the FE phase¹² where $B_2(z)$ modes change into $A_1(z)$ modes due to the transformation from D_{2d} to C_{2v} symmetry at T_c . In the FE phase, Raman spectra also show an additional side

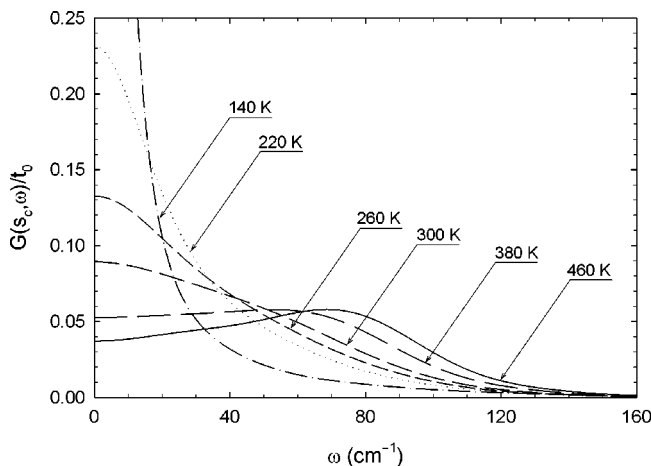


FIG. 2. Spectral densities calculated for $\Gamma_0=26.5 \text{ cm}^{-1}$ along the polar axis of KDP at several temperatures in the paraelectric phase.

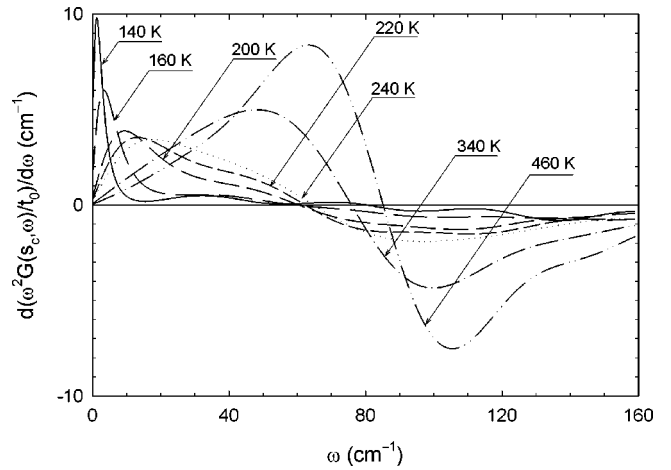


FIG. 3. The first derivative of the spectral densities multiplied by ω^2 calculated for $\Gamma_0=26.5 \text{ cm}^{-1}$ along the polar axis of KDP at several temperatures in the paraelectric phase.

peak (S peak). In the temperature below T_c the CP mode disappears and the S peak remains at about 145 cm^{-1} , exhibiting behavior similar to simulated spectral densities shown in Fig. 1.

The good correlation of experimental Raman spectra of KDP and spectral densities simulated with the MSDPC model was used as a basis for more detailed examination of the central part of the spectrum in the PE phase. As is well known, the central mode is treated as a soft mode and it is responsible for the phase transition in KDP. However, the real structure of the central mode is inconclusive regarding the relaxational or oscillatory nature of the mode and depends on the model involved. Since both of these models can fit the central portion of the Raman spectra, additional considerations of experimental and theoretical evidence are required for a more accurate description of the nature of the phase transition in KDP. In order to resolve possible contributions to the soft mode, the calculated spectral densities are multiplied by the square of the frequency and the first derivative of these functions is shown in Fig. 3. This form is convenient to resolve the oscillatory contributions from the relaxational contributions. The contribution of the harmonic oscillator with frequency ω_0 appears to be positive with a maximum within the frequency interval $(0, \omega_0)$ and changes sign at ω_0 . In contrast, the relaxation contribution described with correlation time τ shows a maximum the position of which is proportional to $1/\tau$, with a positive contribution in the whole frequency interval. Indeed, the two types of contributions are clearly seen in Fig. 3. The high-temperature mode ($460\text{--}220 \text{ K}$) exhibits clear oscillatory character, showing a shift towards low frequencies (from 85 cm^{-1} to 60 cm^{-1}). The second contribution can be seen as a low-frequency peak (below 25 cm^{-1}) at temperatures below 220 K , with a dominant contribution in the positive region of the derivative intensity and a maximum which shifts to zero frequency. Thus, one concludes that the peak shows relaxational and soft mode character. This peak gives a dominant contribution to the spectral density of the whole CP and its temperature dependence can be approximated by the relaxation

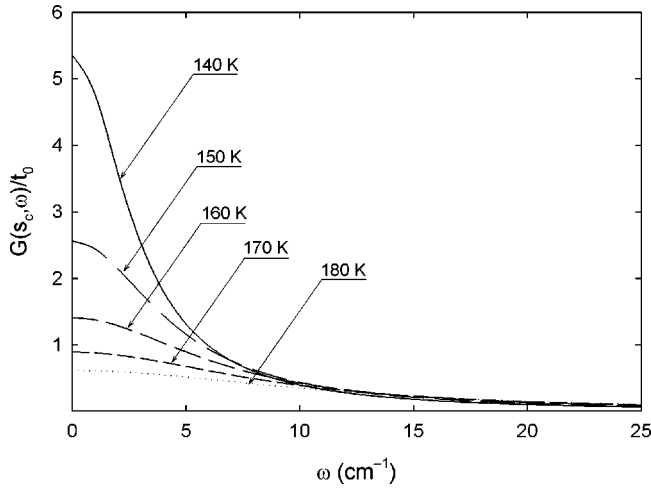


FIG. 4. Spectral densities calculated for $\Gamma_0=26.5 \text{ cm}^{-1}$ along the polar axis of KDP at several temperatures in the vicinity of phase transition, T_c , in the paraelectric phase.

mode function $G_0/(1 + \omega^2\tau^2)$, in accordance with the order-disorder mechanism. The inverse relaxation time $1/\tau$ shows a critical decrease according to the relation from the Ising theory of the order-disorder phase transition¹⁸ in the vicinity of temperature T_0 ,

$$\frac{1}{\tau} = \frac{T - T_0}{\tau_0 T_0}, \quad (7)$$

where τ_0 is an “isolated spin (dipole)” relaxation time. The calculated central peaks below 180 K in the PE-phase, shown in Fig. 4, are fitted to relation (7) and the parameters $T_0 = 128 \pm 2 \text{ K}$ and $\tau_0 = 1.9 \pm 0.1 \times 10^{-13} \text{ s}$ are deduced. The fitted graph is shown in Fig. 5. The calculated points are obtained by employing two different damping constants $\Gamma_0 = 26.5 \text{ cm}^{-1}$ (solid circles) and $\Gamma_0 = 3.3 \text{ cm}^{-1}$ (solid squares) as can be seen in Fig. 5. One notes that the calculated points are independent of the damping constant below temperature $(T - T_0)/T_0 = 0.4$. The independence of the damping constant is expected for the relaxational mode and thus supports the fact that in the temperature region below 180 K the simulated low-frequency peak reflects an order-disorder type of phase transition. It should be noted that in experimentally detected Raman and infrared spectra the similar low-frequency mode with relaxation characteristic was assigned as the f mode^{5,6,19}. Additionally, it can be mentioned that the evaluated τ_0 is in good agreement with $\tau_0 = 1.1 \times 10^{-13} \text{ s}$ obtained from the pulse Raman experiment.⁷

The similar simulation for DKDP (Figs. 6 and 7) shows that the CP and the inelastic peak are well resolved in the whole temperature range. In this case, the CP can be assigned to the relaxational soft mode. The inelastic peak exhibits opposite behavior than that expected for a soft mode: its frequency increases with lowering temperature in the PE phase. Such behavior is in accordance with an order-disorder model where the relaxation mode originates from the jumps between two potential wells and the oscillatory mode is related to oscillations within the potential well minima. It can be noted that good agreement exists between the position of

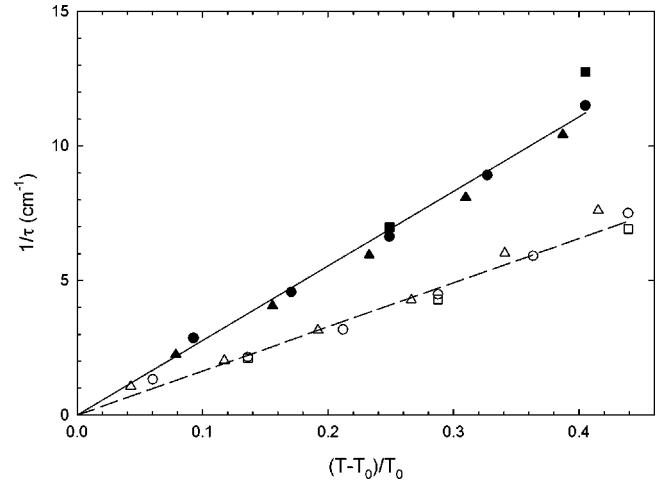


FIG. 5. Temperature dependence of the inverse of relaxation time of the longitudinal polarization in the paraelectric phase for KDP and $N=32$ dipoles; $\Gamma_0=26.5 \text{ cm}^{-1}$ (solid circles) and $\Gamma_0=3.3 \text{ cm}^{-1}$ (solid squares), for DKDP $N=32$ dipoles; $\Gamma_0=26.5 \text{ cm}^{-1}$ (open circles) and $\Gamma_0=3.3 \text{ cm}^{-1}$ (open squares). The obtained data are fitted to relation (7) and shown as a solid line for KDP and as a dashed line for the DKDP lattice. Results for the system of $N=108$ dipoles are shown by solid (KDP) and open (DKDP) triangles.

the lowest experimentally measured²⁰ and calculated oscillatory mode ($110\text{--}160 \text{ cm}^{-1}$) in the FE phase. In the PE phase near T_c , the intensity of the relaxation mode is around three orders of magnitude larger than the intensity of the oscillatory mode and a description of the spectral density with the relaxation mode function, as in the case of KDP, is possible. The parameters $T_0 = 264 \pm 4 \text{ K}$ and $\tau_0 = 3.2 \text{--}0.2 \times 10^{-13} \text{ s}$ are deduced by fitting relation (7) in the temperature region ($T - T_0 < 0.4T_0$). The data are calculated for two different damping constants ($\Gamma_0 = 26.5 \text{ cm}^{-1}$ and $\Gamma_0 = 3.3 \text{ cm}^{-1}$) and presented in Fig. 5. One notes that the fitted data are nearly independent of the damping constant in the monitored temperature region, supporting the relaxation character of the

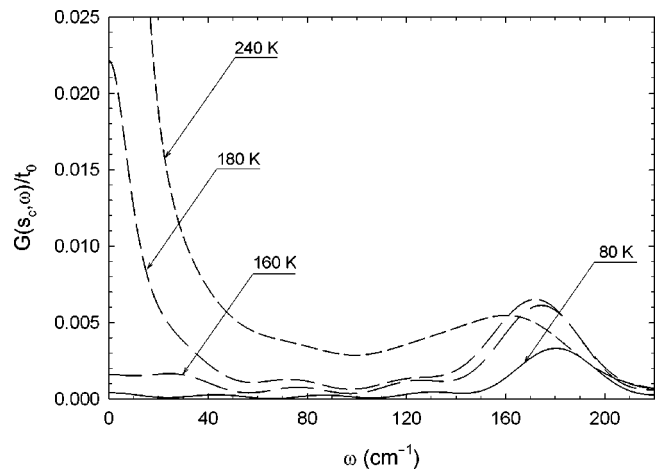


FIG. 6. Spectral densities calculated for $\Gamma_0=26.5 \text{ cm}^{-1}$ along the polar axis of DKDP at several temperatures in the ferroelectric phase.

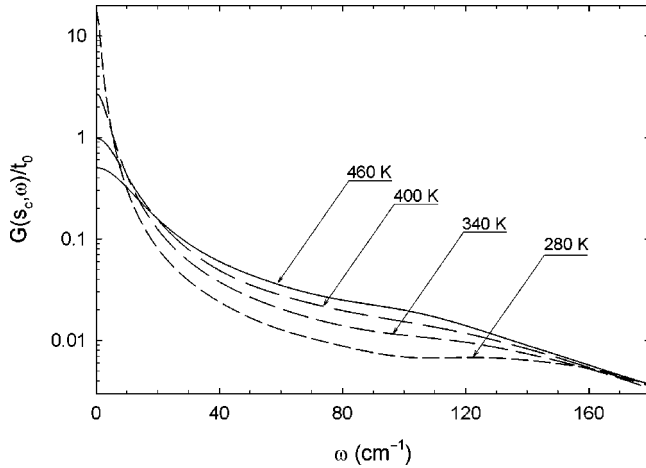


FIG. 7. Spectral densities calculated for $\Gamma_0=26.5 \text{ cm}^{-1}$ along the polar axis of DKDP at several temperatures in the paraelectric phase.

central mode. The influence of the size of the model system on the temperature dependence of CP widths was also examined for both crystals. Simulations were performed on the larger model consisting of $N=108$ dipoles and corresponding to $3 \times 3 \times 3$ unit cells of the crystal. The obtained results are shown in Fig. 5. The newly obtained T_0 and τ_0 parameters coincide (within the same amount of error) with the previous data calculated for the smaller unit cells.

It is shown²¹ that in the random phase approximation of an order-disorder model the single dipole relaxation time τ_0 depends on the local dipole potential—i.e., on the height of the potential barrier V . On the other hand, the phase transition temperature T_c (or T_0) depends on the interaction energy between dipoles. Significantly larger T_0 obtained for the DKDP lattice compared to the KDP lattice is in accordance with the expected shift in T_c for H→D exchange. According to the SDPC model, only the parameter h , which describes an interaction between dipoles [dependent on H (D) mass and geometry of the hydrogen bond], is responsible for the isotope effect in T_0 . One can note that the obtained isotopic ratio for T_0 (~ 2.1) is somewhat larger than the experimental one (~ 1.8). However, by a comparison of τ_0 values obtained for KDP and DKDP, it can be seen that this parameter is also affected by isotopic exchange. This is an important result of the present calculation since the parameter τ_0 is related to a local single-dipole potential. For example, the experimentally measured τ_0 for KDP and DKDP (Ref. 7) shows an even larger ratio (~ 7) than the ratio obtained here (~ 2). Thus, one finds that by changing a single parameter, h , one can change the interaction between the dipoles as well as the depth of the potential wells of the dipole.

It should be mentioned that the dynamical behavior near the critical point could be additionally affected by a direct dipole-dipole (DDD) interaction in accordance with the original SDPC model. As was discussed earlier,⁹ the DDD interaction from the original SDPC model was neglected in the present MSDPC model. This was done in order to emphasize the importance of introducing transversal dipole components, which also interact with protons, and to avoid

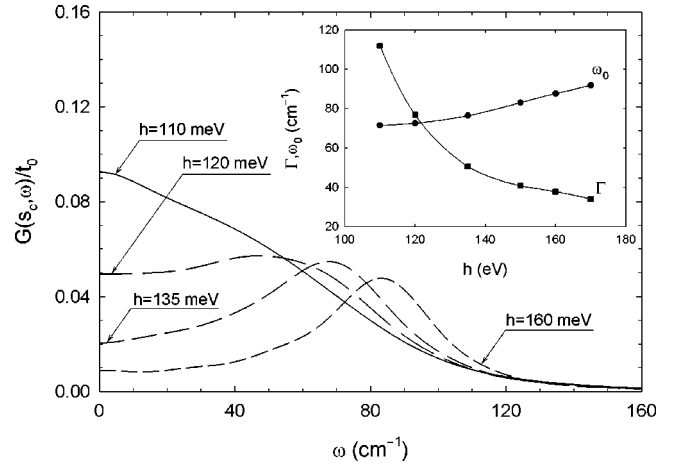


FIG. 8. Spectral densities calculated for several values of the parameter h along the polar axis of KDP at 300 K. The inset shows dependences of ω_0 and Γ on the parameter h .

additional parameters in the model. Thus, in the MSDPC model the whole ferroelectric interaction between the dipoles is due to the isotopic-sensitive interaction via hydrogen bonds. On the contrary, the DDD interaction between longitudinal dipoles—i.e., parameter B in the SDPC—model, is assumed to be insensitive to isotopic exchange. Thus, one expects that the reintroduction of the DDD interaction can reduce the isotopic ratio for T_0 closer to the experimental value.

Moreover, because of the high sensitivity of h to the hydrogen bond length, this parameter may be a good candidate for explanation of the behavior of the CP under pressure. The effect of pressure on the KDP lattice can be explained by the change of h from 110 meV towards larger values. The spectral density was calculated as a function of h at 300 K as shown in Fig. 8. A clear CP structure for the lowest h and the change of this structure to the oscillatory-mode-type structure for other larger h values may be observed. The data shown in Fig. 8 can be fitted to the damped harmonic oscillator, and the influence of h on damping constant Γ and frequency ω_0 is shown in the inset of Fig. 8. The effect of pressure on the CP was measured earlier²² and the change of both Γ and ω_0 is in good qualitative agreement with the predicted behavior due to increasing parameter h in the model. The effect of increasing h is responsible for the decreasing interaction between dipoles as well as for the increasing harmonicity of the local potential, and the dipole excitation in this vicinity should be considered more oscillatory in nature. Furthermore, this effect involves less nonlinearity in the model and affects more the linewidth than the frequency of the simulated soft mode (see inset in Fig. 8). It is important to note that the appearance of inelastic oscillatory modes in the Raman spectra due to increasing pressure on the KDP lattice can be explained within the MSDPC model without including any tunneling effect.

The temperature dependence of the spectral densities for the fluctuation of polarization in a direction perpendicular to the c axis of KDP has been calculated for $\Gamma_0=26.5 \text{ cm}^{-1}$ and is shown in Fig. 9. The high-frequency mode $\omega_0 = \omega_+$

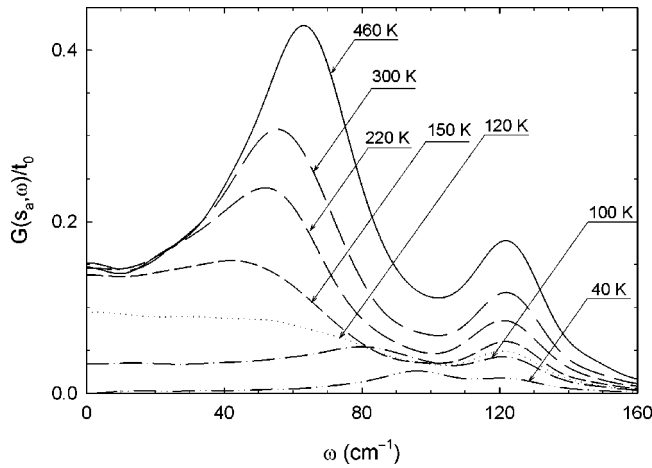


FIG. 9. Spectral densities calculated for $\Gamma_0 = 26.5 \text{ cm}^{-1}$ along the axis perpendicular to the polar axis of KDP at several temperatures.

$= 123 \text{ cm}^{-1}$ and $\Gamma = \Gamma_0 = 26.5 \text{ cm}^{-1}$ (proton dynamics is not included in the mode) exhibits invariant behavior in the whole examined temperature interval (40–460 K). The low-frequency mode (proton dynamics is included in the mode) shows an expected peak at $\omega_- = 100 \text{ cm}^{-1}$ with $\Gamma_0 = 26.5 \text{ cm}^{-1}$ in the low-temperature region. The frequency of the mode shifts to lower frequency values with increasing damping of the mode as temperature approaches T_c in the FE phase. Above T_c the frequency slowly increases from 60 cm^{-1} at 150 K to 70 cm^{-1} at 460 K with decreasing of the damping constant. A mode with such characteristic soft behavior in the PE phase is not experimentally detected. However, the low-frequency spectral density (below 25 cm^{-1}) for $\Gamma_0 = 3.3 \text{ cm}^{-1}$ shows a fast increasing in the FE phase and nearly constant values in the PE phase (Fig. 10). This behavior of the low-frequency region originates from the nonlinear properties of the dipole system and can be qualitatively correlated with the low-frequency flat anomaly experimentally detected in the KDP.^{12,15,23,24}

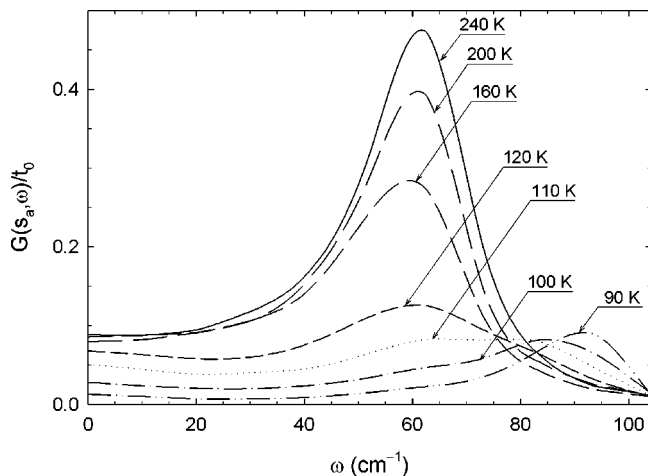


FIG. 10. Spectral densities calculated for $\Gamma_0 = 3.3 \text{ cm}^{-1}$ along the axis perpendicular to the polar axis of KDP at several temperatures.

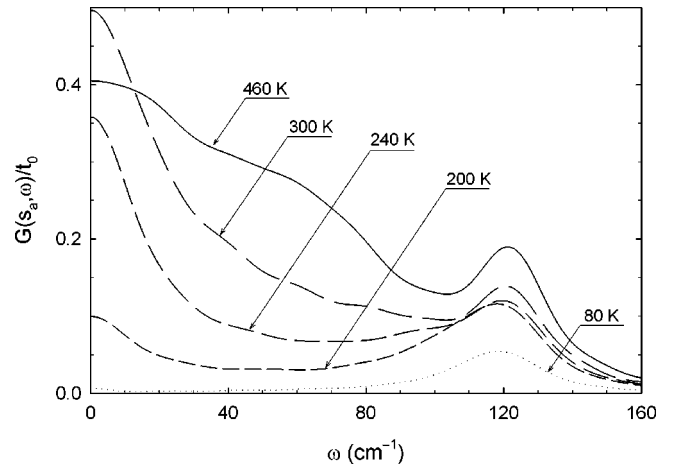


FIG. 11. Spectral densities calculated for $\Gamma_0 = 26.5 \text{ cm}^{-1}$ along the axis perpendicular to the polar axis of DKDP at several temperatures.

Spectral densities of the transversal polarization fluctuation are also simulated for the DKDP lattice by employing $\Gamma_0 = 26.5 \text{ cm}^{-1}$ at various temperatures (Fig. 11). One notes that the low-frequency mode ($\omega_- = 117 \text{ cm}^{-1}$) has a slightly larger frequency than in KDP and it overlaps with the $\omega_+ = 123 \text{ cm}^{-1}$ mode at low temperatures. The CP can be also seen with maximum intensity around 300 K. Above 300 K the intensity of the CP decreases and a broad peak appears around 70 cm^{-1} . The ω_+ mode exhibits the same temperature-independent behavior as in the KDP lattice over the entire temperature interval examined. The oscillatory character of the mode at 70 cm^{-1} in the PE phase is supported by the additional simulation of spectral density for a smaller value of the damping constant ($\Gamma_0 = 3.3 \text{ cm}^{-1}$). A clear narrowing of this mode with the unchanged contribution of the CP mode can be seen in Fig. 12. In Fig. 12 one also notes the narrow ω_+ mode at 123 cm^{-1} , as is expected. Thus, the CP in DKDP can be assigned as relaxation type, indicating the existence of local potential wells along the lateral directions $\pm a$ and $\pm b$. The experimental evidence

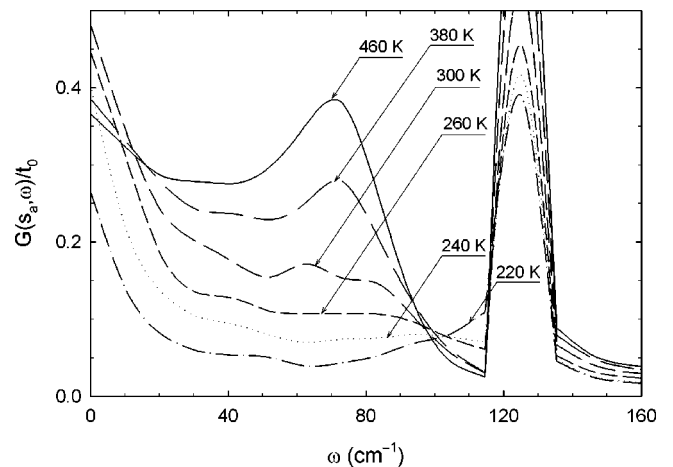


FIG. 12. Spectral densities for $\Gamma_0 = 3.3 \text{ cm}^{-1}$ along the axis perpendicular to the polar axis of DKDP at several temperatures.

for an additional CP mode in the DKDP was detected in E mode Raman¹³ and infrared²⁰ spectra and in dielectric²⁴ measurements. For DKDP as well as for KDP, there is no experimental evidence for the existence of a low-frequency transversal mode with temperature behavior similar to the ω_- mode. However, there is a low-frequency mode at 110 cm^{-1} , which frequency, contrary to other modes, increases in the H \rightarrow D exchange process similar to the ω_- mode.¹³

IV. CONCLUSION

The recently proposed MSDPC model⁹ predicts fairly well the critical behavior of the dielectric constant in the vicinity of the phase transition along the polar axis and along the lateral direction. Therefore, one can extend investigation of the suggested model to the process of the description of dynamical properties of the dipoles in hydrogen-bonded ferroelectrics. Molecular dynamics simulation of the low-frequency modes based on the MSDPC model was studied by employing numerical integration of the classical Langevin equations. The obtained results, in the form of the spectral density of polarization fluctuations along the polar axis and along the lateral direction, are correlated with earlier known experimental data primarily obtained by Raman or infrared spectroscopy on KDP and DKDP lattices. One notes that the model qualitatively predicts most of the expected low-frequency modes in KDP and DKDP lattices. Even more, some of simulated modes show structural features which can be additionally correlated with experimental data.

The properties of the simulated CP in the PE phase have been investigated in order to resolve the character of the soft mode in KDP. It was shown that according to the MSDPC model the soft mode is of oscillatory character at high temperature (460 K). The frequency of the mode softens by decreasing the temperature and, near T_c , an additional relaxation type of mode appears as the soft mode. Thus, the model supports a crossover from the displacive to the order-disorder relaxation mechanism in the PE phase. In the PE phase of DKDP the order-disorder description is valid up to 460 K and τ_0 shows an isotopic effect.

In the FE phase of KDP and DKDP, along with expected inelastic peaks, the CP appears in the calculated spectral density of longitudinal polarization fluctuations as a result of the relaxational mode, in accordance with an order-disorder mechanism.

The model also predicts the low-frequency flat anomaly for KDP and the CP for DKDP in the spectral density of transversal polarization fluctuations as was earlier detected experimentally. Besides these results, the importance of including transversal dipole components in the model seems to be additionally supported by recent preliminary *ab initio* calculations²⁵ for KDP and DKDP. It is shown that unstable modes for the atomic configuration in the PE phase were not only the ferroelectric mode polarized along c , but also two degenerate modes appearing polarized perpendicular to c .

Additionally, the MSDPC model was employed to describe the experimentally measured, pressure-induced change of the CP line shape for KDP at room temperature. The similar change in the CP line shape was reproduced by increasing parameter h in the model (h increases as the hydrogen bond becomes shorter). In the earlier discussion,²² the same experiment was used as important support for a displacive type of phase transition associated with proton tunneling. The above calculation clearly shows that this phenomenon as well as the isotopic effect can be described within the MSDPC model predicting the order-disorder mechanism of the phase transition.

Finally, it is possible to emphasize the difference in the description of central components of longitudinal polarization fluctuations by employing the tunneling model and the MSDPC model. As was mentioned above the tunneling model describes the isotope effect in T_c in the framework of the displacive nature of the phase transition. This was additionally supported by a description of the pressure-induced change of the CP line shape. However, there are three important disagreements between the experimental data and tunneling model predictions: (i) The soft mode below T_c is the CP mode and not the S mode as suggested by the tunneling model. (ii) In the process of H \rightarrow D exchange the S mode shifts to the higher frequencies,¹⁴ opposite to what is expected for deuterated lattices in the tunneling model. (iii) According the pressure experiment the shortening of the hydrogen bond induces an inelastic peak. This inelastic peak appears to be due to a decrease of the soft-mode damping and not due to an increase of the frequency²² as can be expected if this frequency is related to the tunneling frequency.² As was shown above the MSDPC model supports all of these experimental features, showing that the introduction of proton tunneling is not essential for a description of the phase transition in KDP lattices.

¹V.H. Schmidt, *Ferroelectrics* **72**, 157 (1987).

²M. Tokunaga and T. Matsubara, *Ferroelectrics* **72**, 175 (1987).

³R. Blinc, *J. Phys. Chem. Solids* **13**, 204 (1960).

⁴I.P. Kaminow and T.C. Damen, *Phys. Rev. Lett.* **20**, 1105 (1968).

⁵Y. Tominaga and H. Urabe, *Solid State Commun.* **41**, 561 (1982).

⁶S. Shin, Y. Tezuka, S. Saito, Y. Chiba, and M. Ishigame, *J. Phys. Soc. Jpn.* **63**, 2612 (1994).

⁷S. Yoshioka, Y. Tsujimi, and T. Yagi, *Solid State Commun.* **106**, 577 (1998).

⁸H. Sugimoto and S. Ikeda, *Phys. Rev. Lett.* **67**, 1306 (1991).

⁹D. Merunka and B. Rakvin, *Phys. Rev. B* **61**, 11 967 (2000).

¹⁰H. Sugimoto and S. Ikeda, *J. Phys.: Condens. Matter* **6**, 5561 (1994).

¹¹H. Sugimoto and S. Ikeda, *J. Phys.: Condens. Matter* **8**, 603 (1996).

¹²Y. Takagi, *Ferroelectrics* **72**, 67 (1987).

¹³T. Shigenari and Y. Takagi, *J. Phys. Soc. Jpn.* **42**, 1650 (1977)

¹⁴Y. Tominaga, M. Kasahara, H. Urabe, and I. Tatsuzaki, *Solid*

- State Commun. **47**, 835 (1983).
- ¹⁵B. Wyncke and F. Bréhat, J. Phys. C **19**, 2649 (1986).
- ¹⁶A. Agui and Y. Tominaga, J. Phys. Soc. Jpn. **62**, 832 (1993).
- ¹⁷M. Haile, *Molecular Dynamics Simulation* (Wiley, New York, 1992).
- ¹⁸M.E. Lines and A.M. Glass, *Principles and Applications of Ferroelectrics and Related Materials* (Clarendon, Oxford, 1977).
- ¹⁹F. Bréhat and B. Wyncke, Phys. Status Solidi B **128**, 83 (1985).
- ²⁰F. Bréhat and B. Wyncke, J. Phys. C **21**, 4853 (1988).
- ²¹M. Tokunaga and I. Tatsuzaky, Phase Transitions **4**, 97 (1984).
- ²²P.S. Peercy, Phys. Rev. Lett. **31**, 379 (1973).
- ²³P. Simon, F. Gervais, and E. Courtens, Phys. Rev. B **37**, 1969 (1988).
- ²⁴A.A. Volkov *et al.*, Ferroelectrics **25**, 531 (1980).
- ²⁵G. Collizi, J. Kohanoff, and R.L. Migoni, Europhys. Conf. Abstr. **26A**, 6 (2002).